

An innovative fuzzy backstepping sliding mode controller for a Tri-Rotor Unmanned Aerial Vehicle

Shiqian Wang¹ · Jingjuan Zhang¹ · Qian Zhang¹ · Chaoying Pei¹

Received: 16 January 2017 / Accepted: 8 May 2017 / Published online: 18 May 2017
© Springer-Verlag Berlin Heidelberg 2017

Abstract The dynamical model of a Tri-Rotor Unmanned Aerial Vehicle (UAV) is presented in this paper. The Tri-Rotor has three rotors with two fixed-pitch propellers and a tiltable propeller to control the yaw displacement. The model is obtained via the Newton–Euler approach and a nonlinear control strategy called fuzzy backstepping sliding mode control is proposed for the attitude stabilization and altitude tracking of the vehicle. The designed controller consists of a backstepping sliding mode controller and a fuzzy logic controller. For the problem of determining the backstepping sliding mode control coefficients, an optimization method of gradient descent algorithm has been used. However, the control precision of the backstepping sliding mode is intimately dependent on the precision of coefficients. Besides, the uncertain unmodeled coefficients as well as the characteristics of the complex electromechanical system could cause the coefficients not be invariable. Therefore, a fuzzy logic controller is proposed to compensate the coefficients uncertainty to improve the robustness. The effectiveness of the proposed control algorithm is demonstrated via certain simulation results based on the actual parameters of UAV, and its advantages are indicated in comparison with the backstepping sliding mode control without fuzzy logic control.

1 Introduction

The Unmanned Aerial Vehicles (UAV) has been widely used in civil and military applications. The UAV has a variety of potential uses, including search and rescue operations, area mapping, weather monitoring, agricultural operations (Razinkova et al. 2014; Patterson et al. 2014; Salazar-cruz et al. 2008), etc. Vertical take-off and landing (VTOL) vehicle has received a considerable attention and development for several decades (Basri et al. 2015; Tan et al. 2014). A popular class of the VTOL vehicle is multirotor aircraft, which has several lift-generating propellers and does not require a swashplate like helicopter (Basri et al. 2015; Salazar-Cruz et al. 2009). Quadrotor is a common class among different multirotors whose configurations have smaller nonlinear coupling and are easier to control (Escareno et al. 2008). In this paper, we are interested in designing a rotorcraft using only three propellers which has the same manoeuvrability of quadrotor. It is obvious that the advantage of Tri-Rotor over quadrotor is that it requires one motor less which would lead to a reduction of weight, volume and energy consumption (Salazar-Cruz et al. 2009). However, Tri-Rotor has been characterized as with high nonlinearity and complex dynamics, which requires complicated and flexible controllers. In addition, compared with Fixed-Wing aircraft, the model of Tri-Rotor is more sensitive to control inputs, and more susceptible to external disturbance. Thus, it is a challenge to design a Tri-Rotor control system due to these features.

Previously, many control methods have been proposed in the literatures to control a Tri-Rotor aircraft. In (Kara Mohamed and Lanzon 2013) a two stage feedback linearization control method is proposed to handle actuators dynamics and linearise the nonlinear system. In (Rys et al. 2014) and (Czyba et al. 2016) a proportional-integral-derivative

✉ Jingjuan Zhang
jingjuan1002@sina.com

¹ School of Instrument Science and Opto-electronics Engineering, Beihang University, Beijing 100191, China

(PID) control strategy is used to design and control a single tilt Tri-Rotor aerial vehicle. In (Chiou et al. 2013) the focus is on designing a controller based on fuzzy logic to execute hovering tasks efficiently. And in (Anwar et al. 2016) a fuzzy-based hybrid controller is adopted to achieve better transient performance and fast convergence towards stability. A novel sliding mode control strategy is designed for fault-tolerant control in (Yang et al. 2017). Backstepping control is implemented in (Sanca et al. 2014; Kulhare et al. 2012; Song et al. 2016) to deal with nonlinearities, measurement disturbances, noise and sensor biases, furthermore to stabilize the system. The controllers above are simple to implement. However, model uncertainty would cause performance degradation or instability of the control system.

In this paper, a fuzzy backstepping sliding mode controller is used for stabilization and trajectory tracking of Tri-Rotor aircraft. The backstepping control techniques have been widely used in nonlinear system because of their systematic and recursive design methodology for nonlinear feedback control (Fei et al. 2015; Petit et al. 2015; Wang and Wu 2015). Backstepping can force a nonlinear system to behave like a linear system in a new set coordinates in the absence of uncertainties. However, the backstepping controller is always based on the assumption that the structure of the system model is known with unknown slow-varying system parameters. But in actual situation, such as transient performance, unmodeled dynamics, disturbances and not linear parameterizable uncertainties often complicate the control approach. Sliding mode controller is proposed as a systematic method to maintain the stability of Tri-Rotor and achieve consistent performance despite modelling imprecisions. However, backstepping sliding mode controller essentially needs to choose proper coefficients in order to get a satisfactory performance response. The improper coefficients can lead to inappropriate responses (Basri et al. 2014). In this paper, the coefficients of backstepping sliding mode controller are obtained through an optimization method of gradient descent algorithm. To improve disturbance rejection capability of the controller, a fuzzy logic controller is proposed to compensate the coefficients uncertainty.

The work presented in this paper focuses on the Tri-Rotor depicted in Fig. 1. The two main rotors fixed to the aircraft frame in the forward part rotate in opposite directions, decreasing the reaction torque generated to almost zero. By using a servomechanism, the rear rotor can be tilted to produce a yaw torque. The remainder of this paper is organized as follows: In Sect. 2 the mathematical model is presented. The proposed fuzzy backstepping sliding mode control method is described in Sect. 3. Section 4 is devoted to the presentation and the discussion of simulation results with the proposed method applied to the Tri-Rotor. Finally, conclusion and future studies are provided in Sect. 5.



Fig. 1 The Tri-Rotor aircraft

2 Dynamical model

2.1 Definition of coordinate system

Figure 2 is the schematic of the Tri-Rotor. In most cases, a Tri-Rotor UAV is assumed as a rigid object. The coordinate systems are defined as follows: $O_b - X_b Y_b Z_b$ is the body frame. O_b , is at the center of gravity, X_b pointing to the right of the aircraft, Y_b pointing front and Z_b pointing up. $O_n - X_n Y_n Z_n$ is the navigation frame which coincides with the geographic frame (east, north, upwards). $O_{m1} - X_{m1} Y_{m1} Z_{m1}$, $O_{m2} - X_{m2} Y_{m2} Z_{m2}$, $O_{m3} - X_{m3} Y_{m3} Z_{m3}$ are the motor frames which are fixed with three motors, respectively. O_b is the original point of the Tri-Rotor aircraft and the coordinate is $(0, 0, 0)^T$. Therefore, the coordinate of right motor is $(L_1, n, h)^T$, the left one's is $(-L_1, n, h)^T$ and the rear one's is $(0, -l, h)^T$.

2.2 Translational dynamics

The equation of motion for a rigid body object to body force $F^n \in R^3$ applied at the center of mass is given by Newton equation with respect to the navigation coordinate frame and can be written as

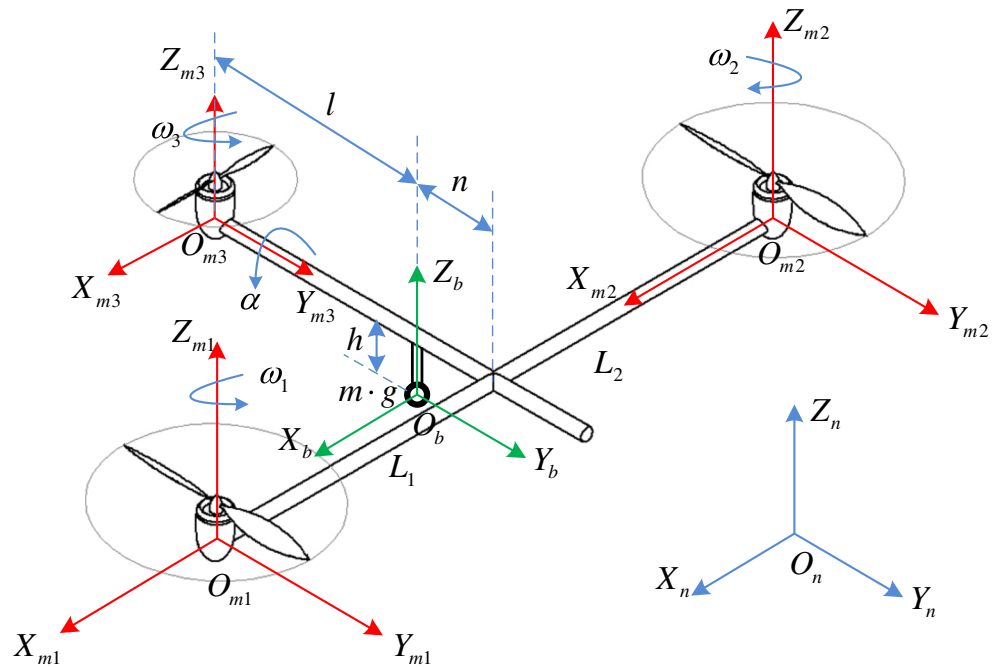
$$m \dot{\vec{V}} = F^n, \quad (1)$$

where $\vec{V} \in R^3$ is the navigation velocity vector, $m \in R$ is the mass of Tri-Rotor.

The thrusts of right and left motors can be defined as $T_1^{m1} = (0, 0, T_1)^T$ and $T_2^{m2} = (0, 0, T_2)^T$, respectively. Translate the thrusts vector into body frame

$$\begin{cases} T_1^b = C_{m1}^b T_1^{m1} \\ T_2^b = C_{m2}^b T_2^{m2} \end{cases} \quad (2)$$

Fig. 2 Schematic of the Tri-Rotor



where $C_{m1}^b = \begin{pmatrix} 1 & 0 & 0 \\ 0 & 1 & 0 \\ 0 & 0 & 1 \end{pmatrix}, C_{m2}^b = \begin{pmatrix} 1 & 0 & 0 \\ 0 & 1 & 0 \\ 0 & 0 & 1 \end{pmatrix}.$

The thrust of rear motor can be defined as $T_3^{m3} = (0, 0, T_3)^T$, translate the thrust vector into body frame $T_3^b = C_{m3}^b T_3^{m3},$ (3)

where $C_{m3}^b = \begin{pmatrix} \cos \alpha & 0 & -\sin \alpha \\ 0 & 1 & 0 \\ \sin \alpha & 0 & \cos \alpha \end{pmatrix},$ α is the tilt angle of rear motor.

The gravity can be defined as $G^n = (0, 0, -mg)^T$ and the resultant force in navigation frame can be described as

$F^n = C_b^n (T_1^b + T_2^b + T_3^b) + G^n,$ (4)

where

$$C_b^n = \begin{pmatrix} \cos \psi & \sin \psi & 0 \\ -\sin \psi & \cos \psi & 0 \\ 0 & 0 & 1 \end{pmatrix} \begin{pmatrix} 1 & 0 & 0 \\ 0 & \cos \theta & \sin \theta \\ 0 & -\sin \theta & \cos \theta \end{pmatrix} \begin{pmatrix} \cos \gamma & 0 & -\sin \gamma \\ 0 & 1 & 0 \\ \sin \gamma & 0 & \cos \gamma \end{pmatrix}$$

$$= \begin{pmatrix} \cos \psi \cos \gamma + \sin \psi \sin \theta \sin \gamma & \sin \psi \cos \theta & -\cos \psi \sin \gamma + \sin \psi \sin \theta \cos \gamma \\ -\sin \psi \cos \gamma + \cos \psi \sin \theta \sin \gamma & \cos \psi \cos \theta & \sin \psi \sin \gamma + \cos \psi \sin \theta \cos \gamma \\ \cos \theta \sin \gamma & -\sin \theta & \cos \theta \cos \gamma \end{pmatrix}.$$

Thus, the full expression of translational dynamic equations is defined as

$$\begin{cases} m\ddot{x} = -T_3 \cdot \sin \alpha \cdot (\cos \psi \cos \gamma + \sin \psi \sin \theta \sin \gamma) + (T_1 + T_2 + T_3 \cos \alpha) \cdot (-\cos \psi \sin \gamma + \sin \psi \sin \theta \cos \gamma) \\ m\ddot{y} = -T_3 \cdot \sin \alpha \cdot (-\sin \psi \cos \gamma + \cos \psi \sin \theta \sin \gamma) + (T_1 + T_2 + T_3 \cos \alpha) \cdot (\sin \psi \sin \gamma + \cos \psi \sin \theta \cos \gamma) \\ m\ddot{z} = -T_3 \cdot \sin \alpha \cdot \cos \theta \sin \gamma + (T_1 + T_2 + T_3 \cos \alpha) \cdot \cos \theta \cos \gamma - mg \end{cases} \quad (5)$$

2.3 Rotational dynamics

In this subsection all the major torques acting on the vehicle in order to derive the angular acceleration equations of motion are presented. The equation of motion for a rigid body object to body torque $M^b \in R^3$ applied at the center of mass is given by Euler equation with respect to the body coordinate frame and can be written as

$I\dot{\omega} + \omega \times I\omega = M^b,$ (6)

where $I \in R^3$ is an inertia matrix and $\omega \in R^3$ is the body angular velocity vector.

Replace $\omega \in R^3$ with vehicle's principle angular acceleration pitch ($\ddot{\theta}$), roll ($\ddot{\gamma}$) and yaw ($\ddot{\psi}$) and considering the vehicle's principle axis inertia (I_{xx}, I_{yy} and I_{zz}), the Eq. 6 can be redefined as

$$\begin{cases} I_{xx}\ddot{\theta} + (I_{zz} - I_{yy})\dot{\gamma}\dot{\psi} = M_x^b \\ I_{yy}\ddot{\gamma} + (I_{xx} - I_{zz})\dot{\theta}\dot{\psi} = M_y^b \\ I_{zz}\ddot{\psi} + (I_{yy} - I_{xx})\dot{\theta}\dot{\gamma} = M_z^b \end{cases} \quad (7)$$

where M_x^b, M_y^b and M_z^b are the components of vector M^b .

As mentioned above, the coordinates of three motors are $d_1 = (L_1, n, h)^T$, $d_2 = (-L_1, n, h)^T$ and $d_3 = (0, -l, h)^T$. So the torques which are derived based on the thrusts of three motors can be defined as

$$\begin{aligned} M_F^b &= T_1^b \times d_1 + T_2^b \times d_2 + T_3^b \times d_3 \\ &= \begin{pmatrix} 0 & -T_1 & 0 \\ T_1 & 0 & 0 \\ 0 & 0 & 0 \end{pmatrix} \begin{pmatrix} L_1 \\ n \\ h \end{pmatrix} + \begin{pmatrix} 0 & -T_2 & 0 \\ T_2 & 0 & 0 \\ 0 & 0 & 0 \end{pmatrix} \begin{pmatrix} -L_2 \\ n \\ h \end{pmatrix} \\ &\quad + \begin{pmatrix} 0 & -T_3 \cos \alpha & 0 \\ T_3 \cos \alpha & 0 & T_3 \sin \alpha \\ 0 & -T_3 \sin \alpha & 0 \end{pmatrix} \begin{pmatrix} 0 \\ -l \\ h \end{pmatrix} \\ &= \begin{pmatrix} -(T_1 + T_2) \cdot n + T_3 \cos \alpha \cdot l \\ T_1 \cdot L_1 - T_2 \cdot L_2 + T_3 \sin \alpha \cdot h \\ T_3 \sin \alpha \cdot l \end{pmatrix}. \end{aligned} \quad (8)$$

As the blades rotate, they are subject to drag forces which produce torques in opposite direction relative to angular velocity of motor. The propeller torques can be defined as $M_1^{m1} = (0 \ 0 \ -Q_1)^T$, $M_2^{m1} = (0 \ 0 \ Q_2)^T$ and $M_3^{m3} = (0 \ 0 \ -Q_3)^T$. These torques can be written in body frame as

$$\begin{aligned} M_R^b &= C_{m1}^b M_1^{m1} + C_{m2}^b M_2^{m2} + C_{m3}^b M_3^{m3} \\ &= \begin{pmatrix} Q_2 \sin \alpha \\ 0 \\ Q_2 - Q_1 - Q_3 \cos \alpha \end{pmatrix}, \end{aligned} \quad (9)$$

where Q_i is the propeller torque.

The gyroscope moment would be created when the rear motor tilts. The gyroscope moment is defined by the cross product of the kinetic moment of the propeller and the tilt velocity vector.

$$\begin{aligned} M_G^b &= C_{m3}^b (H_3^{m3} \times \vec{\alpha}) \\ &= \begin{pmatrix} -J_3 \omega_3 \dot{\alpha} \cos \alpha \\ 0 \\ -J_3 \omega_3 \dot{\alpha} \sin \alpha \end{pmatrix}, \end{aligned} \quad (10)$$

where $H_3^{m3} = (0, 0, J_3 \omega_3)^T$ is the moment vector of momentum and J_3 is the moment of inertia of rear motor. The angular velocity vector of the rear motor is $\vec{\alpha} = (0, \dot{\alpha}, 0)^T$.

Finally, the complete expression of the torque vector, with respect to O_b expressed in body frame is

$$\begin{aligned} M^b &= M_F^b + M_T^b + M_R^b + M_G^b \\ &= \begin{pmatrix} -(T_1 + T_2) \cdot n + T_3 \cos \alpha \cdot l + Q_3 \sin \alpha - J_3 \omega_3 \dot{\alpha} \cos \alpha \\ T_1 \cdot L_1 - T_2 \cdot L_2 + T_3 \sin \alpha \cdot h \\ T_3 \sin \alpha \cdot l + Q_2 - Q_1 - Q_3 \cos \alpha - J_3 \omega_3 \dot{\alpha} \sin \alpha \end{pmatrix}. \end{aligned} \quad (11)$$

Replace all torque expressions in Eq. 6 and the equation of motion can be written as:

$$\begin{cases} I_{xx}\ddot{\theta} + (I_{zz} - I_{yy})\dot{\gamma}\dot{\psi} = -(T_1 + T_2) \cdot n + T_3 \cos \alpha \cdot l \\ \quad + Q_3 \sin \alpha - J_3 \omega_3 \dot{\alpha} \cos \alpha \\ I_{yy}\ddot{\gamma} + (I_{xx} - I_{zz})\dot{\theta}\dot{\psi} = T_1 \cdot L_1 - T_2 \cdot L_2 + T_3 \sin \alpha \cdot h \\ I_{zz}\ddot{\psi} + (I_{yy} - I_{xx})\dot{\theta}\dot{\gamma} = T_3 \sin \alpha \cdot l + Q_2 - Q_1 \\ \quad - Q_3 \cos \alpha - J_3 \omega_3 \dot{\alpha} \sin \alpha \end{cases} \quad (12)$$

3 Control strategy

Backstepping sliding mode control is a technique providing a recursive method of designing stabilizing controls for a class of nonlinear systems that are transformable to a strict feedback system while maintaining stability and consistent performance despite modelling imprecision. In this fuzzy backstepping sliding mode control system, the backstepping sliding mode technique is the main controller, and the coefficients compensation controller containing a fuzzy control approach is used to eliminate the effect of uncertainties caused by external disturbance and unmodeled dynamics.

The state space model for the proposed Tri-Rotor mechanism can be written as follows with state vector X and input vector U :

$$X = [\theta \ \dot{\theta} \ \gamma \ \dot{\gamma} \ \psi \ \dot{\psi} \ x \ \dot{x} \ y \ \dot{y} \ z \ \dot{z}]^T \quad (13)$$

$$U = [u_1 \ u_2 \ u_3 \ u_4 \ u_5 \ u_6]^T, \quad (14)$$

where

$$\begin{cases} u_1 = -(T_1 + T_2) \cdot n + T_3 \cos \alpha \cdot l + Q_3 \sin \alpha - J_3 \omega_3 \dot{\alpha} \cos \alpha \\ u_2 = T_1 \cdot L_1 - T_2 \cdot L_2 + T_3 \sin \alpha \cdot h \\ u_3 = T_3 \sin \alpha \cdot l + Q_2 - Q_1 - Q_3 \cos \alpha - J_3 \omega_3 \dot{\alpha} \sin \alpha \\ u_4 = -T_3 \cdot \sin \alpha \cdot (\cos \psi \cos \gamma + \sin \psi \sin \theta \sin \gamma) + (T_1 + T_2 + T_3 \cos \alpha) \cdot (-\cos \psi \sin \gamma + \sin \psi \sin \theta \cos \gamma) \\ u_5 = -T_3 \cdot \sin \alpha \cdot (-\sin \psi \cos \gamma + \cos \psi \sin \theta \sin \gamma) + (T_1 + T_2 + T_3 \cos \alpha) \cdot (\sin \psi \sin \gamma + \cos \psi \sin \theta \cos \gamma) \\ u_6 = -T_3 \cdot \sin \alpha \cdot \cos \theta \sin \gamma + (T_1 + T_2 + T_3 \cos \alpha) \cdot \cos \theta \cos \gamma - mg \end{cases} \quad (15)$$

Therefore, the vehicle’s state-space model is given by

$$f(X, U) = \begin{bmatrix} \dot{\theta} \\ \dot{\gamma}\dot{\psi}a_1 + b_1u_1 \\ \dot{\gamma} \\ \dot{\theta}\dot{\psi}a_2 + b_2u_2 \\ \dot{\psi} \\ \dot{\theta}\dot{\gamma}a_3 + b_3u_3 \\ \dot{x} \\ b_4u_4 \\ \dot{y} \\ b_5u_5 \\ \dot{z} \\ b_6u_6 \end{bmatrix}, \tag{16}$$

Where $a_1 = \frac{I_{yy}-I_{zz}}{I_{xx}}$, $a_2 = \frac{I_{zz}-I_{xx}}{I_{yy}}$, $a_3 = \frac{I_{xx}-I_{yy}}{I_{zz}}$, $b_1 = \frac{1}{I_{xx}}$, $b_2 = \frac{1}{I_{yy}}$, $b_3 = \frac{1}{I_{zz}}$ and $b_4 = b_5 = b_6 = \frac{1}{m}$.

Considering the first two states subsystem in Eq. 16 for the pitch control as follows

$$\begin{cases} \dot{x}_1 = x_2 = \dot{\theta} \\ \dot{x}_2 = \dot{\gamma}\dot{\psi}a_1 + b_1u_1 \end{cases} \tag{17}$$

Assuming that the target value of pitch angle is θ_d , then the tracking error e_1 and its derivative \dot{e}_1 are considered as follows

$$\begin{cases} e_1 = \theta_d - \theta \\ \dot{e}_1 = \dot{\theta}_d - \dot{\theta} \end{cases} \tag{18}$$

Here, the Lyapunov function is introduced to stabilize the tracking error e_1

$$V(e_1) = \frac{1}{2}e_1^2 \tag{19}$$

$$\dot{V}(e_1) = e_1(\dot{\theta}_d - \dot{\theta}). \tag{20}$$

If the pitch angular velocity $\dot{\theta}$ is considered to be the control input, the pitch angular velocity can be selected as $\dot{\theta} = \dot{\theta}_d + \lambda_1 e_1$ and the Lyapunov function is negative definite.

$$\dot{V}(e_1) = -\lambda_1 e_1^2 < 0. \tag{21}$$

However, the pitch angular velocity $\dot{\theta}$, which is just a system variable, not an actually control input, that can be regarded as a virtual control input and its tracking error could be depicted as

$$S_\theta = \lambda_1 e_1 + \dot{\theta}_d - \dot{\theta}. \tag{22}$$

In addition, the augmented Lyapunov function is $V(e_1, S_\theta) = \frac{1}{2}(e_1^2 + S_\theta^2)$.

Considering the analysis above, the equation $\dot{S}_\theta S_\theta < 0$ should be satisfied. Then choose the attractive surface is the time derivation of Eq. 22

$$\dot{S}_\theta S_\theta = -k_1 \text{sgn}(S_\theta) \cdot S_\theta - \lambda_1 S_\theta^2 < 0. \tag{24}$$

Then the control input can be calculated from equation

$$\begin{aligned} \dot{S}_\theta &= -k_1 \text{sgn}(S_\theta) - \lambda_1 S_\theta \\ &= \lambda_1 \dot{e}_1 + \ddot{\theta}_d - \ddot{\theta} \\ &= \lambda_1(x_2 - \dot{\theta}_d) - \ddot{\theta}_d + a_1 x_4 x_6 + b_1 u_1 \end{aligned} \tag{25}$$

$$u_1 = \frac{1}{b_1}[-a_1 x_4 x_6 + \ddot{\theta}_d - k_1 \text{sgn}(S_\theta) - \lambda_1^2 e_1 - 2\lambda_1 \dot{e}_1]. \tag{26}$$

As is analyzed above, the dynamic sliding mode functions are depicted as follows

$$\begin{cases} S_\theta = \lambda_1 e_\theta + \dot{e}_\theta \\ S_\phi = \lambda_2 e_\phi + \dot{e}_\phi \\ S_\psi = \lambda_3 e_\psi + \dot{e}_\psi \\ S_x = \lambda_4 e_x + \dot{e}_x \\ S_y = \lambda_5 e_y + \dot{e}_y \\ S_z = \lambda_6 e_z + \dot{e}_z \end{cases}, \tag{27}$$

where $e_\theta = \theta_d - \theta$, $e_\phi = \phi_d - \phi$, $e_\psi = \psi_d - \psi$, $e_x = x_d - x$, $e_y = y_d - y$ and $e_z = z_d - z$. Then the stabilizing control laws are as follows

$$\begin{cases} u_1 = \frac{1}{b_1}[-a_1 x_4 x_6 + \ddot{\theta}_d - \lambda_1^2 e_\theta - 2\lambda_1 \dot{e}_\theta - k_1 \text{sgn}(S_\theta)] \\ u_2 = \frac{1}{b_2}[-a_2 x_2 x_6 + \ddot{\phi}_d - \lambda_2^2 e_\phi - 2\lambda_2 \dot{e}_\phi - k_2 \text{sgn}(S_\phi)] \\ u_3 = \frac{1}{b_3}[-a_3 x_2 x_4 + \ddot{\psi}_d - \lambda_3^2 e_\psi - 2\lambda_3 \dot{e}_\psi - k_3 \text{sgn}(S_\psi)] \\ u_4 = \frac{1}{b_4}[\ddot{x}_d - \lambda_4^2 e_x - 2\lambda_4 \dot{e}_x - k_4 \text{sgn}(S_x)] \\ u_5 = \frac{1}{b_5}[\ddot{y}_d - \lambda_5^2 e_y - 2\lambda_5 \dot{e}_y - k_5 \text{sgn}(S_y)] \\ u_6 = \frac{1}{b_6}[\ddot{z}_d - \lambda_6^2 e_z - 2\lambda_6 \dot{e}_z - k_6 \text{sgn}(S_z) - g] \end{cases} \tag{28}$$

In conventional backstepping method, the control law coefficients (λ_i and k_i) are selected by trial and error. To overcome this drawback and identify the values in a convenient way, the gradient descent optimization technique is used, which adjusts the control law coefficients searched using the negative gradient, and attaches an inertia term to achieve a fast convergence to the global minimum (Sheng and Zhang 2015). In this paper, the following function is utilized to judge the performance of the controller:

$$J = \frac{1}{2}(r(k+1) - y(k+1))^2 = \frac{1}{2}e^2(k+1), \tag{29}$$

Table 1 Observer coefficients

Coefficients	λ_1	λ_2	λ_3	λ_4	λ_5	λ_6	k_1	k_2	k_3	k_4	k_5	k_6
Value	30	35	30	28	28	28	1	1	1	1.5	1.5	1.5

where $r(k + 1)$ is the input order and $y(k + 1)$ is the output signal.

In pitch channel, for example, the updated value of parameter λ_1 can be indicated as:

$$\Delta\lambda_1(k + 1) = -\tau \frac{\partial J}{\partial \lambda_1} + \eta \Delta\lambda_1(k), \tag{30}$$

where τ is the learning rate and η is the inertia coefficient. The $\frac{\partial J}{\partial \lambda_1}$ can be calculated as:

$$\frac{\partial J}{\partial \lambda_1} = \frac{\partial J}{\partial y(k + 1)} \cdot \frac{\partial y(k + 1)}{\partial u_1(k)} \cdot \frac{\partial u_1(k)}{\partial \lambda_1(k)}. \tag{31}$$

As the $\frac{\partial y(k+1)}{\partial u_1(k)}$ is associated with dynamics function of the system and it cannot be accurately expressed, so we use sign function $\text{sgn}\left(\frac{\partial y(k+1)}{\partial u_1(k)}\right)$ instead. Thus, the parameter λ_1 can be calculated as follow:

$$\Delta\lambda_1(k + 1) = e(k + 1) \text{sgn}\left(\frac{\partial y(k + 1)}{\partial u_1(k)}\right) \cdot \frac{1}{b_1} [-a_1 x_4 x_6 + \ddot{\theta}_d - 2\lambda_1 e_\theta - 2\dot{e}_\theta - k_1 \text{sgn}(S_\theta)]. \tag{32}$$

The others parameters can be calculated as aforementioned discussion. The gain values for the control law are given in Table 1. However, uncertain unmodeled parameters and complex electromechanical system lead to control errors. It is vital to estimate the effect of the unknown coefficients online and compensate control laws. To handle this problem we apply fuzzy logic control.

Intelligent fuzzy logic control is new and mostly attended area in controller design last decades, and it has been implemented on various dynamical systems (Norton et al. 2015; Yadav and Gaur 2014). Here, the tracking error e and deviation \dot{e} are regarded as the input of the fuzzy controller and control law error is the output. The triangular type is selected as the membership function of inputs and gaussian type is selected as the membership function. The fuzzy logic control sets have been demonstrated in Figs. 3, 4 and 5. The control surface is illustrated in Fig. 6.

Table 2 shows the rules for the fuzzy logic control with two inputs and five linguistic values.

In Figs. 3, 4, the inputs of the fuzzy controller have been normalized to a range of $(-1, +1)$. The expressions of the input normalization are as follows:

$$e_n = \frac{1}{e_{\max}} e \tag{33}$$

$$\dot{e}_n = \frac{1}{\dot{e}_{\max}} \dot{e}. \tag{34}$$

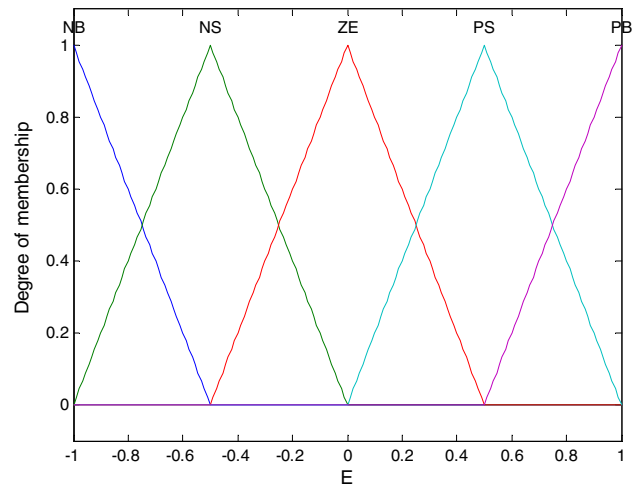


Fig. 3 Membership function of e

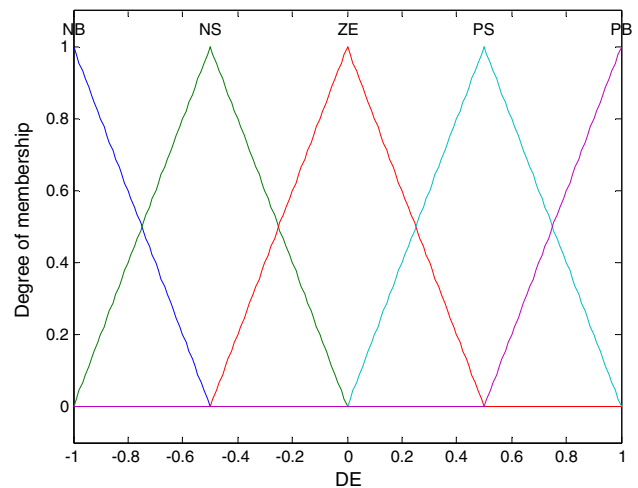


Fig. 4 Membership function of \dot{e}

Similarly, the output of fuzzy controller u_f is denormalized to u_F by the output denormalization factor k_u . The expression of the output denormalization is as follows:

$$u_F = k_u u_f. \tag{35}$$

Then, the improved control law can be represented as:

$$u_{i(I)} = u_i + u_F. \tag{36}$$

In order to guarantee the stability of the system, the output denormalization factor k_u can be calculated as follows:

Consider the Lyapunov function 23–25. Substituting the improved control law Eq. 36, then Eq. 24 becomes:

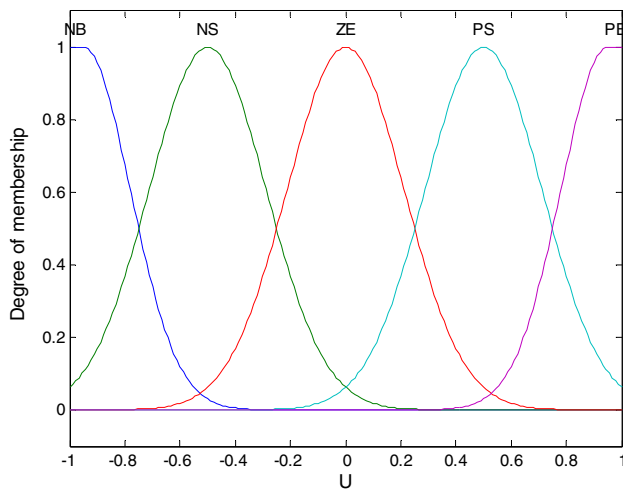


Fig. 5 Membership function of output

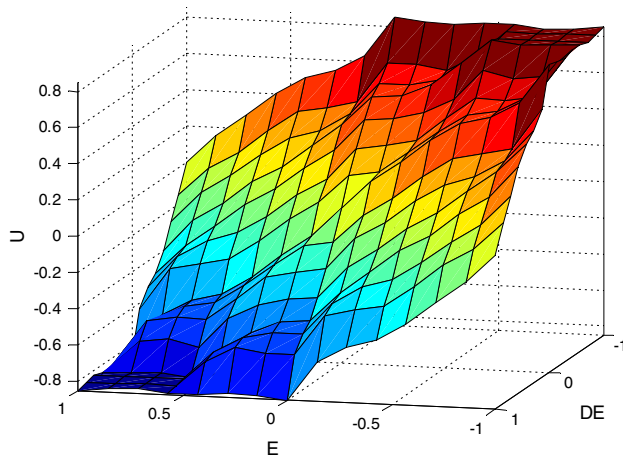


Fig. 6 Designed fuzzy logic surface

$$\dot{S}_\theta S_\theta = (\dot{S}_\theta + b_1 k_u u_f) \cdot S_\theta < 0 \tag{37}$$

$$[b_1 k_u u_f - k_1 \text{sgn}(S_\theta)] \cdot S_\theta - \lambda_1 S_\theta^2 < 0. \tag{38}$$

As $k_1 > 0, \lambda_1 > 0$, if $-k_1 < b_1 k_u u_f < k_1$, the Equation F can be guaranteed.

The output fuzzy sets are normalized in the interval $(-1, +1)$, then $|u_f| \leq 1$, therefore, by choosing $k_u < \frac{k_1}{|b_1|}$ we can make sure the system will be asymptotically stable.

4 Simulation results

In this section, simulation results are presented in order to observe the effectiveness of the derived model and the performances of the proposed fuzzy backstepping sliding mode control law. The simulation results are based on the following real parameters of the Tri-Rotor depicted in Fig. 1. The detailed description has been shown in Table 3.

The control laws $u_{i(t)}$ have been calculated in Sect. 3, the actual control variables can be calculated by inverse solving the Eq. 15. Considering the parameters of the vehicle in Table 3, the expressions of the actual control variables are as follows:

$$\begin{cases} T_1 = -1.25u_1 + 1.25u_2 + 0.025u_4 + 0.4375u_6 + 5.6224 \\ T_2 = -1.25u_1 - 1.25u_2 - 0.025u_4 + 0.4375u_6 + 5.6224 \\ T_3 = 2.5u_1 + 0.125u_6 + 1.6063 \\ \alpha = u_4 / (2.5u_1 + 0.125u_6 + 1.6064) \end{cases} \tag{39}$$

For the purpose of autonomous take-off and landing, the altitude and attitude of the UAV are important control

Table 3 Parameters of the vehicle

Parameter	Mean	Value	Unit
m	Mass	1.31	kg
I_{xx}	Pitch inertia	0.031	kg · m ²
I_{yy}	Roll inertia	0.025	kg · m ²
I_{zz}	Yaw inertia	0.042	kg · m ²
L_1	Position of right motor	0.4	m
L_2	Position of left motor	0.4	m
l	Position of rear motor	0.35	m
n	Position of rear motor	0.05	m
h	Position of gravity center	0.02	m
g	Gravity	9.81	g · s ⁻²

Table 2 Fuzzy rules of tuning system

		e				
		NB	NS	ZE	PS	PB
\dot{e}	NB	PB	PB	PB	PS	ZE
	NS	PB	PB	PS	ZE	NS
	ZE	PB	PS	ZE	NS	NB
	PS	PS	ZE	NS	NB	NB
	PB	ZE	NS	NB	NB	NB

technology indexes. Therefore, the control objectives are to reach and maintain Tri-Rotor at a certain desired altitude and attitude. The inertial states are given by $\theta_0 = 0$, $\gamma_0 = 0$, $\psi_0 = 0$ and $z_0 = 0$. The desired altitude value was placed at $z_d = 10$. The periodic sinusoidal function is used as a reference to the yaw angle and periodic Cosine function is used as a reference to the roll and pitch. In order to simulate the real situation, interference torque is added at the time of 5 s. The control law without fuzzy logic is chosen as the contrastive method. The tracking effects are shown in Figs. 7, 8, 9 and 10 and tracking errors are shown in Figs. 11, 12, 13 and 14.

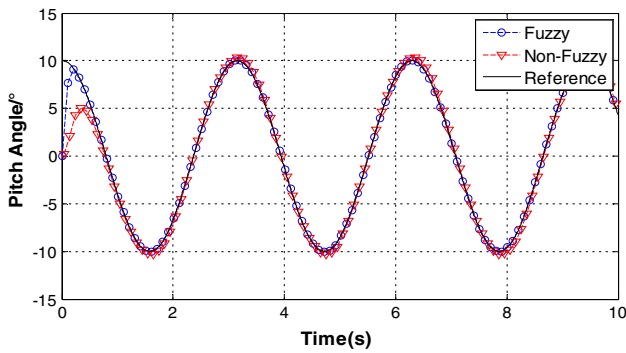


Fig. 7 The tracking effect of pitch angle

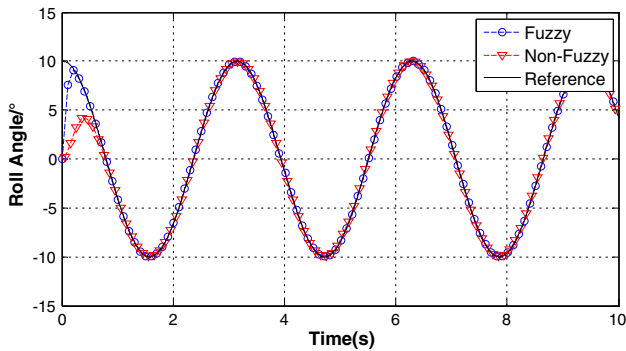


Fig. 8 The tracking effect of roll angle

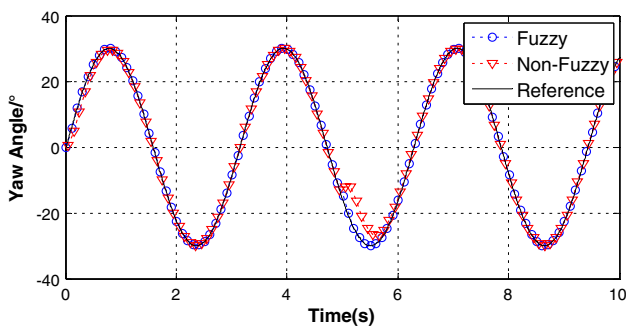


Fig. 9 The tracking effect of yaw angle

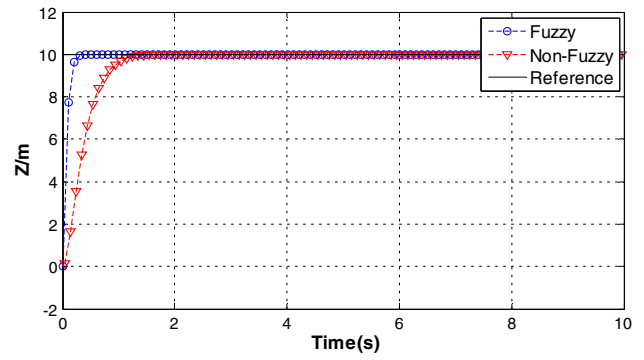


Fig. 10 The tracking effect of altitude

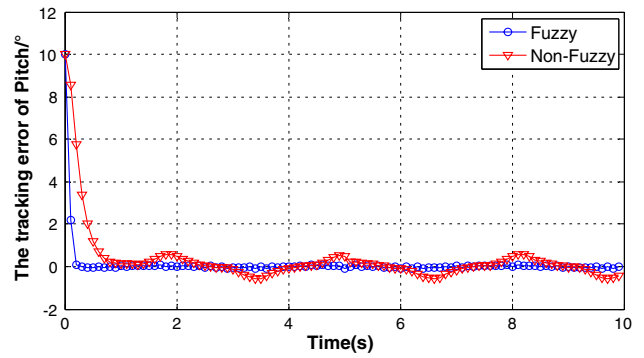


Fig. 11 The tracking error of pitch angle

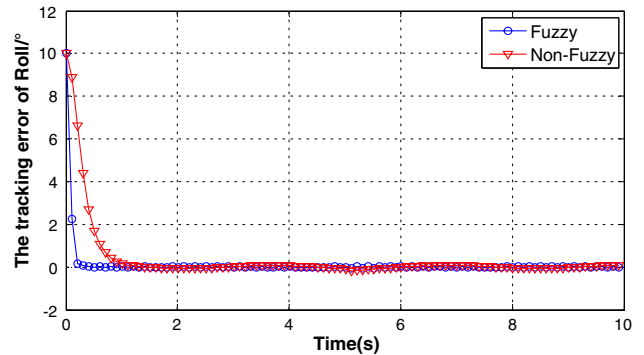


Fig. 12 The tracking error of roll angle

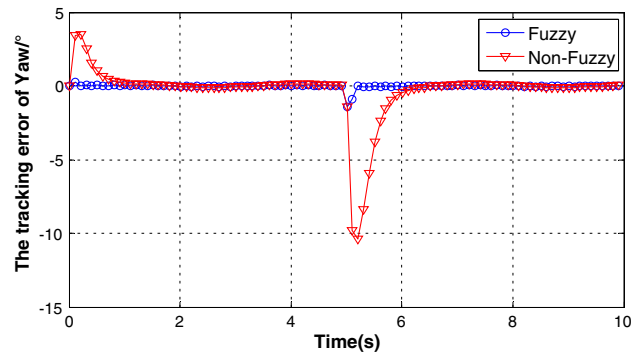


Fig. 13 The tracking error of yaw angle

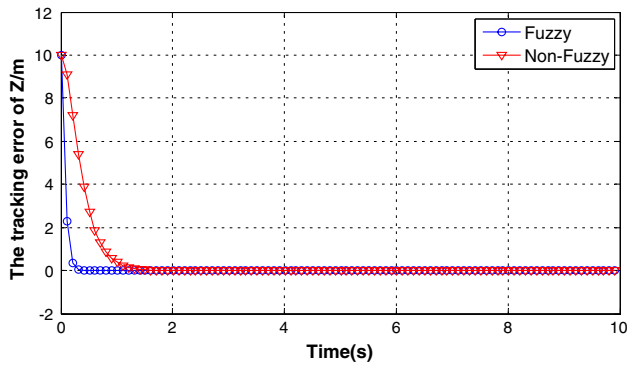


Fig. 14 The tracking error of altitude

Table 4 Fuzzy logic versus non-Fuzzy logic in the tracking error of roll angle

	Settling time (s)	RMS error (°)	Steady-state error (°)
Non-fuzzy logic	0.861	1.548	0.042
Fuzzy logic	0.198	0.661	0.018

Taking Fig. 12 for example, we can see the control improvements with fuzzy logic compared to non-fuzzy logic. Table 4 below has demonstrated the differences in performance via settling time, RMS error and Steady-State error. From Table 4 we can figure out that the RMS error is reduced by 57.2% and the Steady-State error is reduced by 57.1% with fuzzy logic.

The simulation results indicate that the backstepping sliding mode control algorithm is capable of controlling the nonlinear model of the Tri-Rotor. However, at the beginning of simulation, the mutation of states cause the deterioration of the tracking effects. It is obvious that the proposed control law with intelligent fuzzy logic control can achieve a better tracking effect with smaller steady errors. In addition, the improved control algorithm can also speed up the convergence and inhibit the interference torque.

5 Conclusion

This paper has investigated the dynamical model of a Tri-Rotor helicopter and a nonlinear control strategy called fuzzy backstepping sliding mode control which is proposed for the attitude stabilization and altitude tracking of the vehicle. The dynamical model is established by using the traditional Newton–Euler method. Control method designed for such a nonlinear aircraft is a backstepping sliding mode controller which is a powerful nonlinear control method, and useful in controlling flying objects. As

the control precision of the backstepping sliding mode is closely dependent on the precision of coefficients, a fuzzy logic control is proposed to eliminate the coefficients errors and compensate for the coefficients uncertainty. Simulations in this research have been performed to survey the proposed control algorithm. As is shown in the results, the proposed control method can achieve a better tracking effect with smaller steady errors and a faster convergence speed.

References

Anwar AZ, Wang D, Muhammad A (2016) Fuzzy-Based hybrid control algorithm for the stabilization of a tri-rotor UAV. *Sensors* 16(5):652

Basri MAM, Husain AR, Danapalasingam KA (2014) Fuzzy supervisory backstepping controller for stabilization of quadrotor unmanned aerial vehicle. In: 5th international conference on intelligent and advanced systems, Kuala Lumpur, Malaysia, 2014

Basri MAM, Husain AR, Danapalasingam KA (2015a) A hybrid optimal backstepping and adaptive fuzzy control for autonomous quadrotor helicopter with time-varying disturbance. *J Aerosp Eng* 229:2178–2195

Basri MAM, Husain AR, Danapalasingam KA (2015b) GSA-based optimal backstepping controller with a fuzzy compensator for robust control of an autonomous quadrotor UAV. *Aircr Eng Aerosp Technol* 87:493–505

Chiou JS, Tran HK, Peng ST (2013) Attitude control of a single tilt tri-rotor UAV system: dynamic modeling and each channel’s nonlinear controllers design. *Math Probl Eng* 2013:6 doi:10.1155/2013/275905

Czyba R, Szafranski G, Ryś A (2016) Design and control of a single tilt tri-rotor aerial vehicle. *J Intell Robot Syst* 84:1–14

Escareno J, Sanchez A, Garcia O, Lozano R (2008) Triple tilting rotor mini-UAV: modeling and embedded control of the attitude. In: American Control Conference, 2008, pp 3476–3481

Fei JT, Yan WF, Yang YZ (2015) Adaptive nonsingular terminal sliding mode control of MEMS gyroscope based on backstepping design. *Int J Adapt Control Signal Process* 19:1099–1115

Kara Mohamed M, Lanzon A (2013) Effect of unmodelled actuator dynamics on feedback linearised systems and a two stage feedback linearisation method. In: Decision and Control. IEEE, 2013, pp 841–846

Kulhare A, Chowdhury AB, Raina G (2012) A back-stepping control strategy for the tri-rotor UAV. In: China control and decision conference, 2012, pp 3481–3486

Norton M, Khoo S, Kouzani A, Stojcevski A (2015) Adaptive fuzzy multi-surface sliding control of multiple-input and multiple-output autonomous flight systems. *IET Control Theory Appl* 9:587–597

Patterson T, McClean S, Morrow P, Parr G, Luo C (2014) Timely autonomous identification of UAV safe landing zones. *Image Vis Comput* 32:568–578

Petit F, Daasch A, Albu-Schaffer A (2015) Backstepping control of variable stiffness robots. *IEEE Trans Control Syst Technol* 23:2195–2202

Razinkova A, Kang BJ, Cho HC, Jeon HT (2014) Constant altitude flight control for Quadrotor UAVs with dynamic feedforward compensation. *Int J Fuzzy Logic Intell Syst* 14:26–33. doi:10.5391/IJFIS.2014.14.1.26

- Rys A, Czyba R, Szafranski G (2014) Development of control system for an unmanned single tilt tri-rotor aerial vehicle. In: International conference on unmanned aircraft systems, 2014, pp 1091–1098
- Salazar-cruz S, Kendoul F, Lozano R, Fantoni I (2008) Real-Time Stabilization of a Small Three-Rotor Aircraft. *IEEE Trans Aerosp Electron Syst* 44:783–794
- Salazar-Cruz S, Lozano R, Escaren J (2009) Stabilization and nonlinear control for a novel trirotor mini-aircraft. *Control Eng Pract* 17:886–894
- Sanca AS, Alsina PJ, Cerqueira JJF (2014) Stability analysis of a multirotor UAV with robust backstepping controller. In: Joint conference on robotics: Sbr-Lars robotics symposium and robocontrol, 2014, pp 241–246
- Sheng HL, Zhang TH (2015) MEMS-based low-cost strap-down AHRS research. *Measurement* 59:63–72
- Song Z, Li K, Cai Z et al (2016) Modeling and maneuvering control for tricopter based on the back-stepping method. In: guidance, navigation and control conference (CGNCC) In: 2016 IEEE Chinese. IEEE, 2016, pp 889–894
- Tan FX, Liu DR, Guan XP (2014) Online optimal control for VTOL aircraft system based on DHP algorithm. In: Proceedings of the 33rd Chinese control conference, Nanjing, China, 2014, pp 28–30
- Wang YC, Wu HS (2015) Adaptive robust backstepping control for a class of uncertain dynamical systems using neural networks. *Nonlinear Dyn* 81:1597–1610
- Yadav AK, Gaur P (2014) AI-based adaptive control and design of autopilot system for nonlinear UAV Sadhana-Academy. *Proc Eng Sci* 39:765–783
- Yang P, Pan X, Liu J et al (2017) Optimal fault-tolerant control for UAV systems with time delay and uncertainties over wireless network[J]. *Peer-to-Peer Netw Appl* 10(3):717–725